Fatigue Behavior of Variable Loaded Bridge Details Near the Fatigue Limit

PETER B. KEATING AND JOHN W. FISHER

The findings of the current NCHRP Project 12–15(5), "Fatigue Behavior of Variable Loaded Details Near the Fatigue Limit," are highlighted. The main focus of the research is the examination of welded bridge details in the high-cycle, long-life regime. Large-scale plate girders with coverplate, web attachment, and web stiffener details are subjected to fatigue loading that simulates actual truck traffic. A Rayleigh type stress spectrum is used with the inclusion of an occasional overload exceeding the constant-amplitude fatigue limit. The frequencies of occurrence being considered for the overloads are 0.1, 0.05, and 0.01 percent. Prior research indicated that fatigue crack propagation occurred even when the effective stress range was below the constant-amplitude fatigue limit and the exceedance rate of the limit was as low as 0.1 percent. The current test specimens also allow for a detailed study of distortion-induced fatigue cracking at a connection plate web gap detail. Results indicate that the retrofit method of drilled holes at the crack tip is inadequate at high levels of distortion. In addition to the experimental work, a review of fatigue test data generated around the world since the AASHTO fatigue provisions were adopted in 1974 was completed. This study has allowed for a reassessment of the provisions. A summary of the proposed revisions to the specifications is given.

In order to fully understand the fatigue behavior of welded steel bridge members and details, test data resulting from full-scale test specimens must be generated and analyzed. The NCHRP Project 12–15(5) entitled "Fatigue Behavior of Variable Loaded Bridge Details Near the Fatigue Limit," concerns itself with several aspects of full-scale fatigue testing. The primary objective of the research program is to study the fatigue behavior of welded bridge details subjected to variable-amplitude, high-cycle fatigue loading. This type of loading is more representative of what an actual bridge is subjected to than the constant-amplitude loading that has been used to generate almost all of the data that forms the database for the current AASHTO fatigue provisions. In addition, the fatigue behavior of web connection plate details is investigated.

This experimental work is unique in that both crack development and the adequacy of retrofit methods can be examined under variable-amplitude loading and in a laboratory environment. No previous research of this type has been performed. As a supplement to the project, a reassessment of the current fatigue design criteria has been completed. This study involved the compilation of full-scale fatigue test data generated since the introduction of the AASHTO fatigue provisions in 1974. The test data were evaluated to determine the adequacy of the fatigue provisions. Recommendations for change to the fatigue design specifications have been set forth so that the specifications may better reflect the expanded fatigue test database.

Fritz Engineering Laboratory, Lehigh University, Bethlehem, Pa. 18015.

HIGH-CYCLE FATIGUE TESTS

Fatigue cracks developed at the ends of the coverplated bridge beams that were only infrequently subjected to stress ranges that exceeded the fatigue limit of AASHTO's Category E' *(1)*. This suggests that severe fatigue problems could result if bridges become subjected to heavier loads in the future, and that the consequences of occasional overloads from permits and other sources may be more critical than previously assumed. The consequence of initiating fatigue crack growth in existing bridges as a result of increased loads could have a major impact on the life expectancy and safety of bridges on high-volume arteries where large numbers of random variable-stress cycles are expected. The available test data in the high-cycle region of behavior are sparse and do not provide an adequate basis on which to assess this problem. The principal objective of NCHRP Project 12–15(5) is to extend the findings of Project 12–15(4) [NCHRP Report 267 *(2)*] by providing additional information on the fatigue behavior of welded bridge members under randomly applied, variable-amplitude loading near the fatigue limit of the extreme-life region.

Background

Fatigue test results from several studies before the NCHRP 12–15(5) project indicated that fatigue cracks develop in test specimens even though the effective stress range is well below the crack growth threshold or fatigue limit *(3, 4)*. The types of specimens tested varied from small-scale attachment details to full-scale coverplated beams. The percentage of cycles exceeding the constant-amplitude fatigue limit for these tests ranged from 100 percent to as few as 0.24 percent. However, these studies were limited in scope in that only a few detail types were tested, and with those, a limited number of tests were run. This procedure resulted in little or no replication of data.

The NCHRP Project 12–15(4) test program was initiated with the objective to expand the existing database through the use of full-scale beams. Eight rolled W18 × 50 beams of A588 steel with a span length of 15 ft were used. Two types of welded attachments were incorporated: 1- × 4½-in. partial-length coverplates and 1.0-in.-thick by 12.0-in.-long fillet-welded web attachments. All beams were tested in their as-welded state. A Rayleigh type distribution was used for the

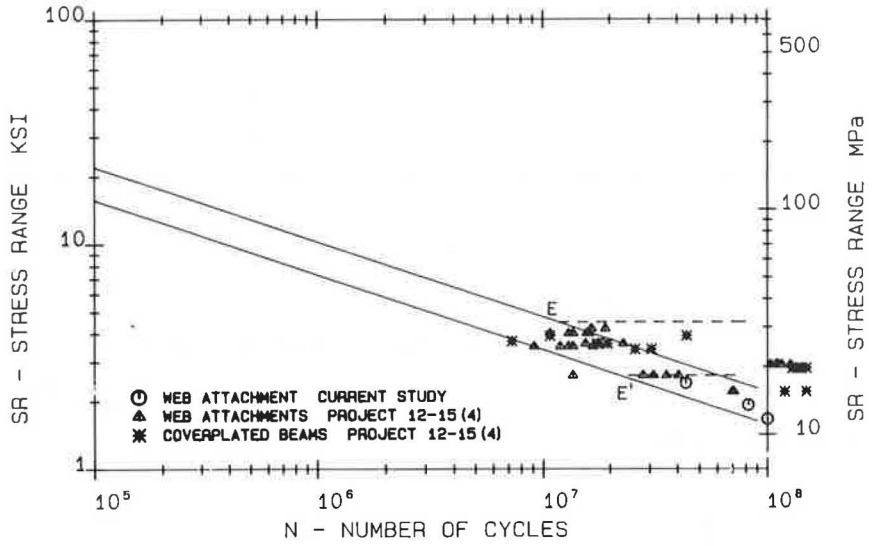

FIGURE 1 Fatigue test data, NCHRP Projects 12–15(4) and 12–15(5).

stress range spectrum. Fatigue limit exceedance rates, held constant for a given test, varied from 0.10 to 11.72 percent for the program.

The test results from Project 12–15(4) are shown in Figure 1. The data are plotted by using the effective stress range as calculated from the root mean cubed (RMC) (Miner's) rule:

$$S_{re} = (\Sigma\, \alpha_i \cdot S_{ri}^3)^{1/3} \quad (1)$$

where S_{re} is the effective stress range, S_{ri} is the stress range at the ith interval of the frequency-of-occurrence histogram, and α_i is the fraction of stress range within the ith interval. All stress cycles in the spectrum are assumed to contribute to fatigue crack propagation. As indicated in the figure, the test data plot consistently with the straight-line extension of the Categories E and E′ design curves even though the calculated effective stress ranges are below the constant-amplitude fatigue limit. The results were revealed to be independent of the exceedance rate. The study concluded that the existence of a fatigue limit below which no fatigue crack propagation occurs is assured only if none of the stress cycles exceed this constant-amplitude fatigue limit.

Research Approach

The current NCHRP Project 12–15(5) involves the fatigue testing of eight full-scale welded plate girders. All webs, flange plates, and attachments are A36 steel. Each girder is 26 ft long; girders are tested in pairs on a 25-ft span under four-point loading. A view of the test setup is shown in Figure 2. The girders are 36 in. deep with 1- × 12-in. flanges and a 3/8-in.-thick web plate. Three detail types are fillet welded to the girders: partial-length coverplates, web attachments, and transverse web stiffeners. The coverplates are 1- × 9-in. plates, either with or without the transverse end weld. This detail provides a Category E′ classification because the flange thickness is greater than 0.8 in. The web attachments consist of 1.0-in.-thick by 12-in.-long plates with longitudinal fillet welds only. These are also Category E′ due to their thickness. The 3/8- ×

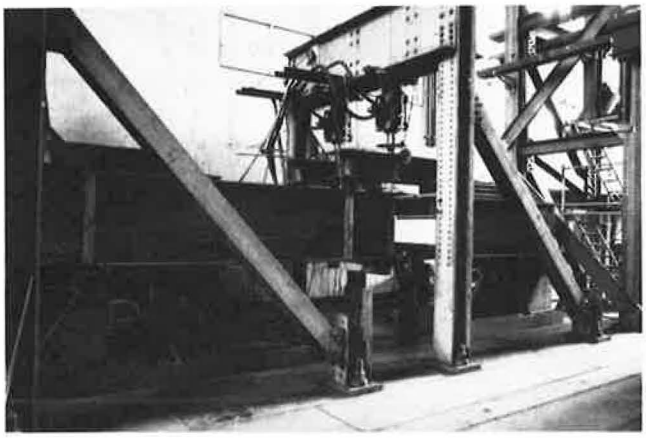

FIGURE 2 View of test setup of full-scale plate girders.

3.0-in. transverse web stiffeners (Category C) are cut short of the tension flange with a 1 1/2-in. web gap. The girder and attachment configurations are shown in Figure 3. Each test girder has 16 possible detail failure locations.

As with previous test programs, a Rayleigh type stress spectrum is used. The variable-amplitude stress spectrum is generated by repeatedly applying a block of 1,000 randomized loads of 10 different magnitudes. The details are arranged on the girder so that each reaches its respective constant-amplitude fatigue limit at the same applied load. The web attachments were arranged in the shear span to provide a range in the assumed constant-amplitude fatigue limit from 4.2 to 2.3 ksi. The 10th or highest load in the spectrum corresponds to the fatigue limit of the detail. A normalized stress range spectrum, which results in an effective stress range 58 percent of the detail fatigue limit, is shown in Figure 4. Overloads are included into the spectrum at set exceedance rates. For the first pair of girders, this rate is 0.1 percent. Subsequent rates will be 0.05 and 0.01 percent. The magnitudes of the overloads result in stress ranges at each detail that are between 7/6 and 3/2 of the assumed constant-amplitude fatigue limit.

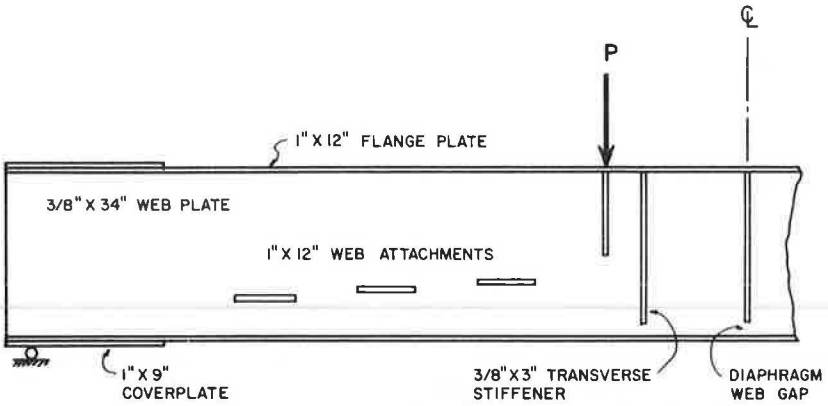

FIGURE 3 Plate girder with welded details.

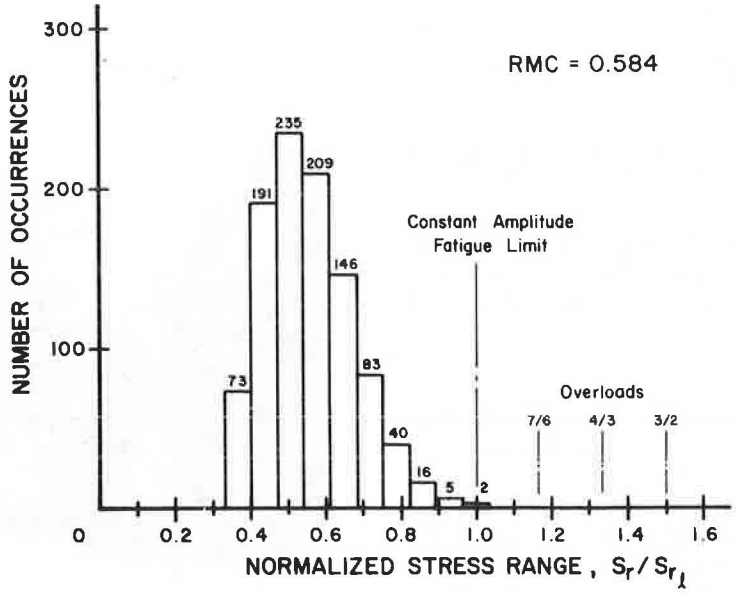

FIGURE 4 Normalized stress range histogram.

Results and Evaluation of Experimental Data

The fatigue test has yielded three failure points, which occurred at the weld end of three web attachments (Figure 5), through the first quarter of 1987. One detail, with an effective stress range of 2.4 ksi, failed at $43.6 \cdot 10^6$ cycles. While the constant amplitude fatigue limit of Category E′ is 2.6 ksi, the position of this particular detail gave an assumed fatigue limit of 4.2 ksi for a 0.1 percent exceedance rate. Using the Category E′ fatigue limit results in an exceedance rate of 14.6 percent. Fatigue crack growth was detected at a second web attachment detail at $81.7 \cdot 10^6$ cycles. At this location, the load spectrum results in an effective stress range of 2.2 ksi with a peak value of 4.3 ksi. The third crack was detected at $100.7 \cdot 10^6$ cycles, at an effective stress range of 1.4 ksi and a maximum stress range of 3.5 ksi. These data points are plotted in Figure 1, as the open circle symbols.

Further fatigue crack growth at this detail was prevented by the placement of holes through the web plate at the crack tips. Different-sized holes were used at each end because the crack resided in a moment stress gradient. Diameters were 1.0 in. for the top and 2.0 in. for the bottom hole. These sizes were selected on the basis of the relationship

$$\Delta K/\sqrt{\rho} = 4\sqrt{\sigma_y} \quad (2)$$

where ΔK ($\sqrt{\text{ksi-in.}}$) is the stress intensity factor range, ρ (in.) is the diameter of the hole, and σ_y (ksi) is the yield stress of the steel *(5)*.

DISTORTION-INDUCED FATIGUE CRACKING

As a secondary study on NCHRP Project 12–15(5), distortion-induced fatigue cracking at a connection plate web gap detail is also being examined under variable-amplitude loading. The current test program presents an opportunity to examine and evaluate this type of fatigue cracking and possible retrofit methods under long-life conditions. Before the project, no other laboratory study of distortion-induced fatigue cracking had simulated in-service loading conditions, that is, both in-plane and out-of-plane stresses simultaneously.

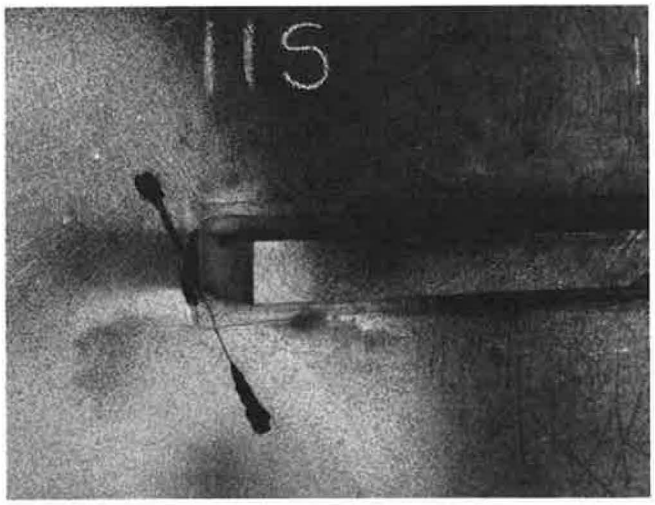

FIGURE 5 Fatigue crack at web attachment.

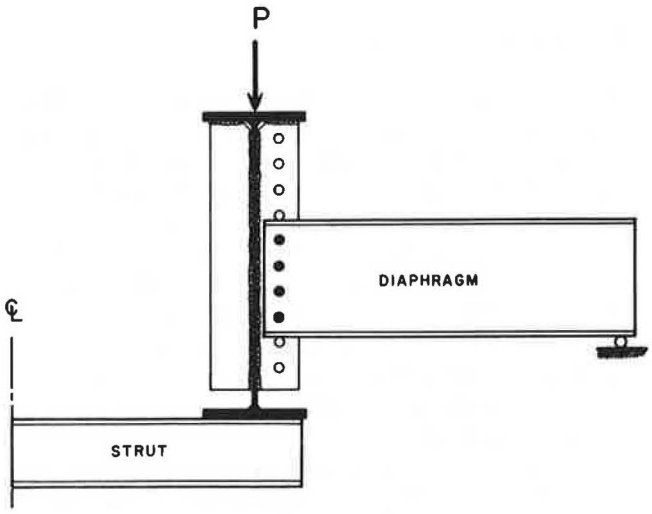

FIGURE 6 Test setup for distortion-induced web gap fatigue cracking.

As shown in Figures 2 and 3, each test girder contains a web gap detail at midspan. The connection plate is cut short of the tension flange by either 1½ or 4 in. A diaphragm consisting of a W14 × 22 rolled section is bolted to the connection plate with its free end supported against vertical motion at the test frame column. This configuration is shown schematically in Figure 6. The bottom flange of the test girder is restrained against rotation by means of a rolled section strut, simulating a flange embedded in a concrete deck or the restraint found at a support. The in-plane vertical deflection of the girder from the applied loads causes the connection plate to be forced out-of-plane by the resisting moment developed at the diaphragm connection. This setup models the differential displacement of bridge girders and the resulting distortion at diaphragm locations in the negative-moment region and at supports.

Strain measurements taken during static tests, before the variable-amplitude loading, indicated that the vertical web gap membrane stresses were high. At the static load that produced an in-plane stress at the connection plate end equivalent to the constant amplitude fatigue limit (12 ksi), a strain corresponding

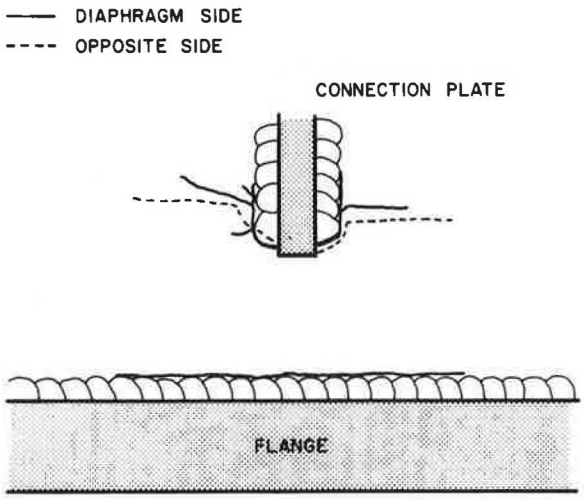

FIGURE 7 Map of the web gap fatigue cracking.

to 43 ksi was measured. This distortion-induced stress is approximately 20 percent greater than the nominal yield stress of the steel. Varying the vertical bolted position of the diaphragm resulted in no significant changes in the measured web gap stresses.

With the onset of variable-amplitude loading, fatigue cracks developed quickly in the web gaps. The initial cracking was first detected at approximately 50,000 cycles, with extensive cracking at 100,000 cycles. The distortion-induced fatigue cracks developed at both the toe of the web-to-flange fillet weld and at the connection plate end as shown schematically in Figure 7.

At approximately 1 million random variable-load cycles, the web gap cracking was retrofitted by means of drilled holes at the crack tips. Figure 8 shows the progression of fatigue cracking in stages at one of the web gap details. Holes of 1½-in. diameter were used to core out the cracking at the connection plate end and ¾-in.-diameter drilled holes were used at the tips of the web-to-flange cracks (Stage I). Within 500,000 cycles, crack reinitiation occurred at the toe of both the connection plate weld and the web-to-flange weld. The crack tips were again arrested by drilling and testing was resumed (Stage II). At $2.1 \cdot 10^6$ cycles (Stage III), and again at $2.9 \cdot 10^6$ cycles (Stage IV), a crack reinitiated at the drilled hole along the stiffener fillet weld toe.

At this point in the test, the diaphragms were permanently removed from the test girders to prevent further distortion-induced fatigue damage and avoid the possible loss of the girders due to fracture at the connection plate detail. Strain measurements taken at the top of the uppermost hole (Stage IV) indicated that the in-plane web stresses were elevated 10 percent because of the presence of the web cracks. Subsequently, a crack reinitiated at the perimeter of the drilled hole at $9.4 \cdot 10^6$ cycles (Stage V). The test was run an additional 20 million cycles before a toe crack reinitiated at the top hole (Stage VI). The crack tip was drilled out and the toe of the vertical fillet weld was peened to help prevent additional cracking. At $47 \cdot 10^6$ cycles (Stage VII), fatigue cracks initiated at the perimeter of the uppermost hole and at one of the web-to-flange holes. The second crack represented a situation that would

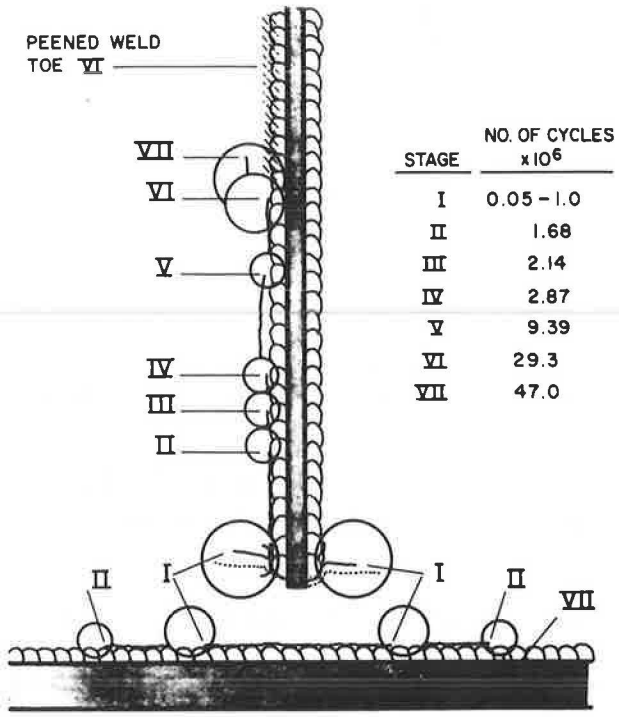

FIGURE 8 Schematic history of web gap fatigue cracking.

eventually jeopardize the test. Strain measurements on the flange plate gave an increase of 12 percent over the nominal stress without the web cracking. The crack front was drilled on both sides of the web plate and the flange plate clamped to help reduce the level of stress in the flange, minimizing the probability of continued cracking. A view of the final stage of web and flange cracking and retrofit holes is given in Figure 9.

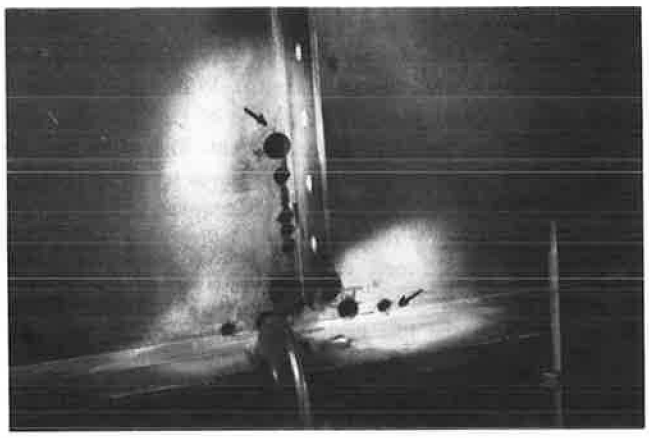

FIGURE 9 Retrofitted distortion-induced web cracking.

This discussion illustrates the difficulty in retrofitting web gap cracking when it is induced by high levels of out-of-plane deformation. Even though holes were drilled at the crack tips, the level of stress from the out-of-plane motion of the diaphragm remained at such an elevated state that cracks quickly reinitiated. When the diaphragms were removed and the in-plane loading continued, the detail had previously sustained such a large magnitude of damage that cracks continued to develop and propagate. Eventually, the web cracks caused the stresses in both the web and flange plates to increase enough to initiate cracking at the perimeter of the holes. Peening stopped the crack from initiating at the weld toe.

FATIGUE DATA REVIEW

A fatigue data review and reassessment of the current fatigue specifications has been conducted *(6)*. Since the AASHTO specification fatigue resistance provisions were developed from test data reported in NCHRP Reports 102 and 147 *(7, 8)*, several major fatigue studies have been conducted around the world. By compiling and reviewing all available full-scale test data, the existing fatigue specifications could be reevaluated and appropriate changes made so that the specifications more accurately reflect the current state of knowledge. In addition, the review provides an opportunity to provide fatigue criteria consistent with applications in other countries.

Background

Before NCHRP Project 12–7 [NCHRP Reports 102 and 147 *(7, 8)*] only approximate fatigue design relationships were in use because of the limitations of the test data available at the time. NCHRP Project 12–7 was developed to provide a statistically designed experimental program under controlled conditions. The program involved some 530 test beams and girders with various welded details that are commonly used in the design of bridges. Large-size beam specimens were used to overcome some of the limitations of smaller, simulated specimens, such as reduced residual-stress fields and limited initial-weld defect distributions. All specimens were tested under constant cycle loading.

The results from the regression analyses of the generated test data indicated that only two variables significantly influenced the fatigue strength of the welded details: stress range and the detail type. Steel type and minimum and maximum stress levels were found to be not significant. This simplification resulted from the presence of residual stresses that exist in welded steel structures from the welding process. A stress–range–cycle–life relationship was defined using six different design categories to classify the fatigue strength of the details used in the test program. This procedure led to the provisions now used in the current AASHTO fatigue design specifications *(9)*.

Research Approach

Data were collected from many different sources around the world, including Japan, Switzerland, East Germany, Office of Research and Experiments of the International Union of Railways—ORE (West Germany, Poland, England, and Holland), as well as the United States. These additional studies evaluated the applicability of the NCHRP test program to fabrication conditions elsewhere in the world and were used to develop similar fatigue codes. The additional tests augmented the NCHRP findings and often defined the fatigue strength of details that were not examined under the NCHRP program.

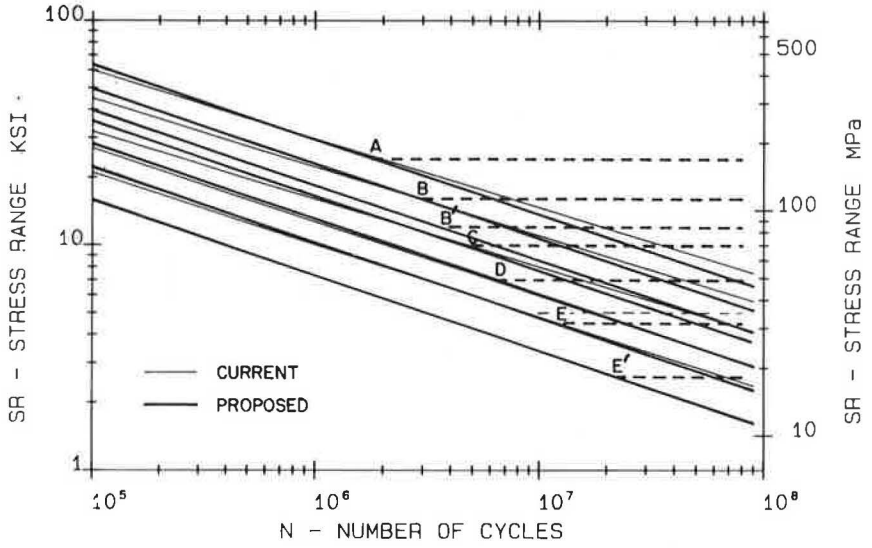

FIGURE 10 Comparison of current and proposed AASHTO design curves.

A major effort of the fatigue test review was the development of a computerized database containing fatigue test results of varying detail types *(10)*. Included in the database were the data from both the original NCHRP test program (to 1972) and from all the new sources. The development of this database allowed for the systematic analysis of the large amount of fatigue data compiled from various references.

The database was limited to test data that could be used to define the fatigue resistance of welded steel details. This limitation meant the inclusion of test data resulting from large-scale test specimens. As was extensively addressed in NCHRP Reports 102 and 147 *(7, 8)*, small-scale specimens always provide higher cycle lives than large-scale beam type specimens. Small-scale specimens were used in the review where no alternative existed, though reliance on these data has been minimal. No attempt was made to evaluate the fatigue strength of riveted and bolted connections. Nor was the adequacy of weld improvement techniques evaluated. While these processes tend to increase the fatigue resistance of certain details, the objective of the review was to accurately define the lower bound resistance for as-welded details, or the minimum level of fatigue strength that would be obtained provided that standard fabrication and inspection procedures were employed.

Each new source of test data was first compared with the appropriate AASHTO fatigue curves to determine if the results from the recent tests were consistent with the findings of the original NCHRP studies or if the fatigue resistance of a particular detail had possibly been misrepresented by the current specifications. A regression analysis was performed using all the data for a given detail type to determine if any significant differences arose. Once the new data were properly categorized, all data, both old and new, for each detail type were compared with the appropriate fatigue resistance curve.

Findings

The reassessment of the fatigue provisions provided an opportunity to have the AASHTO fatigue criteria consistent with

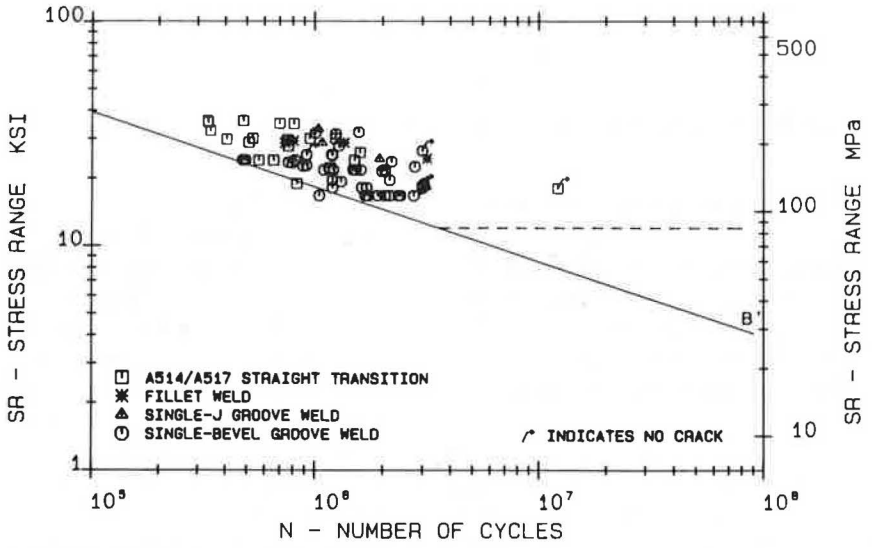

FIGURE 11 Category B′ fatigue test data.

TABLE 1 PROPOSED ALLOWABLE STRESS RANGE VALUES FOR REDUNDANT MEMBERS

Redundant Load Path Members				
	Allowable Range of Stress F_{sr}, ksi			
Category	For 100,000 Cycles	For 500,000 Cycles	For 2,000,000 Cycles	For over 2,000,000 Cycles
A	63	37	24	24
B	49	29	18	16
B	39	23	14.5	12
C	35.5	21	13	10 12
D	28	16	10	7
E	22	13	8	4.5
E′	16	9.2	5.8	2.6
F	15	12	9	8

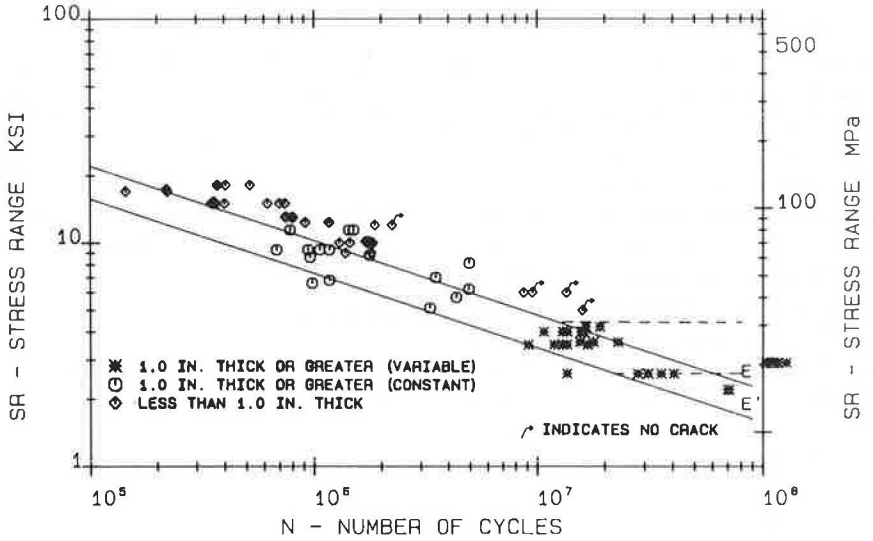

FIGURE 12 Web attachment test data with Category E and E′.

other applications in other countries. As the database for a given detail has increased it has generally been observed that the slope of the S–N curve tends to stabilize to a value of –3.0. Also, recognition of the relationship between crack growth and the experimental results on welded details has led to the adoption of a slope of –3.0 for other design S–N curves, such as those adopted by the European Convention Constructional Steelwork (ECCS) *(11)*.

The results of the present fatigue data review suggested that minor adjustments to the existing AASHTO fatigue design curves were desirable. The slopes of the proposed curves were all established at –3.0. A comparison between the existing and proposed fatigue design curves is shown in Figure 10. With the exception of Category A, the proposed curves were developed by using the current stress range intercept values at $2 \cdot 10^6$ cycles. The constant-amplitude fatigue limit for each curve, with the exception of Category E, corresponds to its current value, as the review of the data did not indicate a need to change these values. A new category, B′, has been added because the review indicated that Category B overestimated the fatigue strength of certain longitudinal groove welds. The stress range intercept values for 100,000, 500,000, and 2,000,000 cycles as well as the constant-amplitude fatigue limits for each proposed curve are given in Table 1.

Fatigue test data obtained from full-scale box girder specimens with longitudinal partial-penetration groove welds indicated a

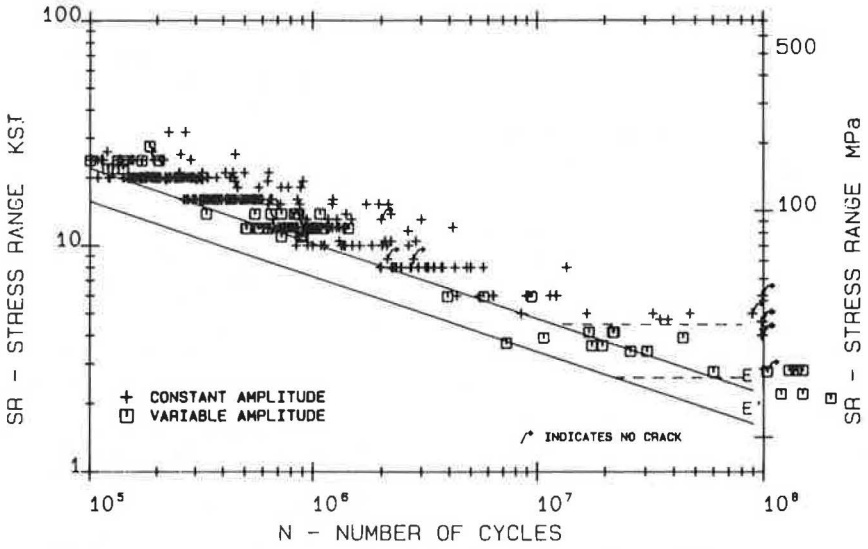

FIGURE 13 Coverplated beam test data with Category E and E′.

TABLE 2 PROPOSED ALLOWABLE STRESS RANGE VALUES FOR NONREDUNDANT MEMBERS

Non-Redundant Load Path Members				
	Allowable Range of Stress F_{sr}, ksi			
Category	For 100,000 Cycles	For 500,000 Cycles	For 2,000,000 Cycles	For over 2,000,000 Cycles
A	50	29	24	24
B	39	23	16	16
B	31	18	11	11
C	28	16	10 12	9 11
D	22	13	8	5
E	17	10	6	2.3
E	12	7	4	1.3
F	12	9	7	6

fatigue strength consistently below Category B *(12–14)*. In Figure 11, these data are plotted with the proposed Category B′ design curve. The decreased resistance is due to the geometry at the detail. Large initial defects were found to occur in the large-scale sections as a result of blowholes and root gap flaws. These defects appear to be larger than the discontinuities observed in full-penetration groove welds and fillet welds. This same condition has been observed in longitudinal groove welds with backing bars left in place. Category B′ has also been recommended to define the fatigue strength of full-penetration groove-welded splices at transitions in width or thickness when the base metal is of A514/A517 steel. These data points are also plotted in Figure 11. Previously, the use of flange splices in A514/A517 steel was permitted only with a 2.0-ft radius transition.

The analysis of the test data for web attachments indicated that the plate thickness has an influence on the fatigue strength of this type of detail *(2, 15)*. Shown in Figure 12 are data for this type of detail, plotted with both the proposed Category E and E′ design curves. The web attachment details with a plate thickness of 1.0 in. or greater resulted in a fatigue resistance that was below Category E. It was revealed that Category E′ gave a more reasonable lower bound estimate of the fatigue resistance of this detail.

High-cycle, long-life fatigue tests of coverplated beams *(16)* indicated that 5.0 ksi overestimated the constant-amplitude fatigue limit for this type of detail. The minimum-stress range value at which fatigue failure occurred was found to be 4.7 ksi. It was concluded that a stress range value of 4.5 ksi was a better estimate of the constant-amplitude fatigue limit for Category E.

The complete database for coverplated beams with a flange thickness less than 0.8 in. is shown in Figure 13.

Concern where failure of a single element could cause collapse of a structure resulted in a more conservative fatigue design requirement in order to minimize the possibility of fatigue crack growth in fracture critical members. In order to provide a rational and consistent criterion for nonredundant members, a uniform reduction of 20 percent has been applied to the allowable stress range values at 100,000, 500,000, and 2,000,000 design cycles. The 20 percent reduction provides uniformly the minimum reduction that was used in the earlier versions of the AASHTO specifications. The reduced allowable stress range values are analogous to designing the structure for a 25 percent higher load. The allowable stress range values for nonredundant load path members are given in Table 2.

Summary

The review of the test data that has been produced since NCHRP Reports 102 and 147 were published has significantly increased the database for welded steel details. New types of details that were not previously covered in the original provisions have been added to the database. The comparison of the test data with the current AASHTO fatigue provisions did not result in any major deviation between the design fatigue strength and the test results. The findings that were reported in the original NCHRP reports have been supported by the subsequent test programs. No indications were given in the more recent studies that the NCHRP results were in error.

CONCLUSIONS

NCHRP Project 12–15(5) has provided the opportunity to study several important aspects of the behavior of welded bridge details using full-scale specimens. The results from the high-cycle fatigue tests allow for a rational assessment of the variable loadings that cross bridge structures so that existing structures can be assessed for possible fatigue damage. The results will be used to assess the adequacy of existing AASHTO fatigue design specifications. The full-scale test specimens have also allowed for the examination of distortion-induced fatigue cracking under variable-amplitude loading at a web gap detail. Preliminary results have indicated that holes drilled at the crack tip are ineffective in arresting the crack propagation at high stress levels. The fatigue data review has resulted in proposed changes to the current AASHTO fatigue design specifications that better reflect the expanded database for fatigue test data of full-scale welded bridge details.

REFERENCES

1. J. W. Fisher, R. E. Slockbower, H. Hausamman, and A. W. Pense. Long Time Observation of a Fatigue Damaged Bridge. *Journal of the Technical Councils of ASCE*, Vol. 107, No. TC1, April 1981, pp. 55–71.
2. J. W. Fisher, D. R. Mertz, and A. Zhong. *NCHRP Report 267: Steel Bridge Members Under Variable Amplitude Long Life Fatigue Loading*. TRB, National Research Council, Washington, D.C., 1983.
3. C. G. Schilling, K. H. Klippstein, J. M. Barsom, and G. T. Blake. *NCHRP Report 188: Fatigue of Welded Steel Bridge Members Under Variable-Amplitude Loading*. TRB, National Research Council, Washington, D.C., 1978.
4. P. Albrecht and I. M. Friedland. Fatigue Limit Effect on Variable-Amplitude Fatigue of Stiffeners. *Journal of the Structural Division, ASCE*, Vol. 105, No. ST12, Dec. 1979, pp. 2657–2675.
5. J. W. Fisher, B. M. Barthelemy, D. R. Mertz, and J. A. Edinger. *NCHRP Report 227: Fatigue Behavior of Full-Scale Welded Bridge Attachments*. TRB, National Research Council, Washington, D.C., 1980.
6. P. B. Keating and J. W. Fisher. *NCHRP Report 286: Evaluation of Fatigue Tests and Design Criteria on Welded Details*. TRB, National Research Council, Washington, D.C., 1986.
7. J. W. Fisher, K. H. Frank, M. A. Hirt, and B. M. McNamee. *NCHRP Report 102: Effects of Weldments on the Fatigue Strength of Steel Beams*. TRB, National Research Council, Washington, D.C., 1970.
8. J. W. Fisher, P. A. Albrecht, B. T. Yen, D. J. Klingerman, and B. M. McNamee. *NCHRP Report 147: Fatigue Strength of Steel Beams with Welded Stiffeners and Attachments*. TRB, National Research Council, Washington, D.C., 1974.
9. *Standard Specifications for Highway Bridges*, 13th ed., AASHTO, Washington, D.C., 1983.
10. P. B. Keating, S. A. Halley, and J. W. Fisher. *Fatigue Test Database for Welded Steel Bridge Details*. Fritz Engineering Laboratory Report 488.2(86). Lehigh University, Bethlehem, Pa., May 1986.
11. *Recommendations for the Fatigue Design of Structures, Committee TC6 Fatigue*, 1st ed., European Convention for Constructional Steelwork, Brussels, Belgium, 1985.
12. C. Miki, T. Nishimura, J. Tajima, and A. Okukawa. Fatigue Strength of Steel Members Having Longitudinal Single-Bevel-Groove Welds. *Trans. of Japan Welding Society*, Vol. 11, No. 1, April 1980, pp. 43–56.
13. C. Miki, F. Nishino, J. Tajima, and Y. Kishimoto. Initiation and Propagation of Fatigue Cracks in Partially-Penetrated Longitudinal Welds. *Proc. of Japan Society of Civil Engineers*, No. 312, Aug. 1981, pp. 129–140.
14. *ORE Report D 130—Fatigue Phenomena in Welded Connections of Bridges and Cranes*. Reports D130/RP 1/E through D130/RP 10/E. Office of Research and Experiments of the International Union of Railways, Paris, France.
15. J. W. Fisher, H. Hausamman, M. D. Sullivan, and A. W. Pense. *NCHRP Report 206: Detection and Repair of Fatigue Damage in Welded Highway Bridges*. TRB, National Research Council, Washington, D.C., 1979.
16. R. F. Slockbower and J. W. Fisher. *Fatigue Resistance of Full Scale Cover-Plated Beams*. Fritz Engineering Laboratory Report 386–9(78), Lehigh University. Bethlehem, Pa., 1978.

Publication of this paper sponsored by Committee on Steel Bridges.